Annotating Enzymes of Unknown Function: *N*-Formimino-L-glutamate Deiminase Is a Member of the Amidohydrolase Superfamily†

Ricardo Martí-Arbona, Chengfu Xu, Sondra Steele, Amanda Weeks, Gabriel F. Kuty, Clara M. Seibert, and Frank M. Raushel*

Department of Chemistry, P.O. Box 30012, Texas A&M University, College Station, Texas 77842-3012

Received December 13, 2005; Revised Manuscript Received January 2, 2006

ABSTRACT: The functional assignment of enzymes that catalyze unknown chemical transformations is a difficult problem. The protein Pa5106 from *Pseudomonas aeruginosa* has been identified as a member of the amidohydrolase superfamily by a comprehensive amino acid sequence comparison with structurally authenticated members of this superfamily. The function of Pa5106 has been annotated as a *probable* chlorohydrolase or *cytosine deaminase*. A close examination of the genomic content of *P. aeruginosa* reveals that the gene for this protein is in close proximity to genes included in the histidine degradation pathway. The first three steps for the degradation of histidine include the action of HutH, HutU, and HutI to convert L-histidine to *N*-formimino-L-glutamate. The degradation of *N*-formimino-L-glutamate to L-glutamate can occur by three different pathways. Three proteins in *P. aeruginosa* have been identified that catalyze two of the three possible pathways for the degradation of *N*-formimino-L-glutamate. The protein Pa5106 was shown to catalyze the deimination of *N*-formimino-L-glutamate to ammonia and *N*-formyl-L-glutamate, while Pa5091 catalyzed the hydrolysis of *N*-formyl-L-glutamate to formate and L-glutamate. The protein Pa3175 is dislocated from the hut operon and was shown to catalyze the hydrolysis of *N*-formimino-L-glutamate to formamide and L-glutamate. The reason for the coexistence of two alternative pathways for the degradation of *N*-formimino-L-glutamate in *P. aeruginosa* is unknown.

The pace by which the complete DNA sequence of whole genomes can be determined is rapidly accelerating. This explosion in the total number of available gene sequences has dramatically unveiled the evolutionary relationships within broadly dispersed enzyme superfamilies (*1*, *2*). Protein sequence comparisons have clearly shown that new functions have evolved from existing enzyme templates through the process of divergent evolution (*2*−*4*). However, the functional annotation for many genes in both prokaryotic and eukaryotic organisms is *uncertain*, *unknown*, or *incorrect* (*5*−*8*). This fact suggests that a considerable amount of fundamental biological chemistry remains to be discovered. However, the discovery of function for enzymes that catalyze reactions with unidentified substrates is a rather difficult problem. Nevertheless, the substrate and reaction diversity within a given enzyme superfamily can provide considerable information for the assignment of function for those enzymes with ambiguous substrates.

The amidohydrolase superfamily is a functionally diverse group of enzymes, and members of this superfamily are found in every organism sequenced to date (*9*, *10*). The structural landmark for this superfamily is a mononuclear or binuclear metal center embedded within the confines of an $(\alpha/\beta)_8$-barrel structural fold (*4*). Most of the enzymes within this superfamily catalyze the hydrolysis of oxygen or nitrogen bonds to carbonyl or phosphoryl centers. Some of the more prominent enzymes in this superfamily include urease, phosphotriesterase, adenosine deaminase, and dihydroorotase. At least 30 different reactions have been catalogued for members of this superfamily, and it has been estimated that perhaps as many as another 100 substrates remain to be determined (*4*, *10*).

In the databases maintained by the NCBI,[1] a significant fraction of those members of the amidohydrolase superfamily with unknown function are annotated as *probable chlorohydrolases* or *probable cytosine deaminases*. This assignment is based upon the apparent sequence similarity to enzymes that catalyze the hydrolysis of the carbon−chlorine bond in atrazine or the hydrolysis of the carbon−nitrogen bond in cytosine as illustrated in the reactions presented in Scheme 1. One of these genes (Pa5106; gi:15600299) is found within the genome of *Pseudomonas aeruginosa* PA01 (*11*). Amino acid sequence comparisons with the entire set of completely and partially sequenced microbial genomes find 38 other genes with an overall sequence identity of greater than 40%. Many of these enzyme homologues are functionally annotated as probable chlorohydrolases. The likelihood that all of these microorganisms have evolved an enzyme for the degradation of the herbicide atrazine seems relatively remote.

† This work was supported in part by the NIH (GM 71790 and GM 33894) and the Robert A. Welch Foundation (A-840).

* To whom correspondence may be sent. Tel: (979)-845-3373. Fax: (979)-845-9452. E-mail: raushel@tamu.edu.

[1] Abbreviations: NCBI, National Center for Biotechnology Information; HutH, histidine ammonia lyase; HutU, urocanase; HutI, imidazolone propionate amidohydrolase; HutF, *N*-formimino-L-glutamate deiminase; HutG, *N*-formyl-L-glutamate amidohydrolase; ATCC, American Type Culture Collection; HEPES, *N*-2-hydroxyethylpiperazine-*N*′-2-ethanesulfonic acid; PMSF, phenylmethylsulfonyl fluoride; IPTG, isopropyl-thiogalactoside; CDA, cytosine deaminase; ADA, adenosine deaminase; AtzA, atrazine chlorohydrolase.

10.1021/bi0525425 CCC: $33.50
Published on Web 01/31/2006

Scheme 1: Reactions Catalyzed by Atrazine Chlorohydrolase and Cytosine Deaminase

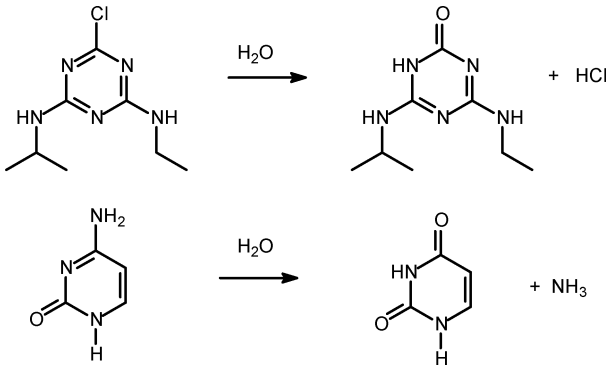

Curiously, an examination of the genomic context for these genes within this subset of amidohydrolase enzymes reveals that in nearly every instance these genes are found adjacent to a cluster of other genes that are involved in the degradation of histidine. This suggests that perhaps this subgroup of amidohydrolase superfamily enzymes is directly involved in the degradation of histidine. The genomic environment of the histidine degradation locus in *P. aeruginosa* is shown in Figure 1.

The pathway for the degradation of histidine has been studied in a number of organisms (*12*). The first three steps for the catabolism of histidine are similar in most species. Histidine is first deaminated to urocanate by histidine ammonia lyase (HutH); urocanase (HutU) converts this product to imidazolone-4-propionate, and then HutI (imidazolone propionate amidohydrolase) catalyzes the cleavage of the imidazolone ring to *N*-formimino-L-glutamate. The degradation of *N*-formimino-L-glutamate can apparently occur by three different independent pathways (*13*). The formimino group can be transferred to tetrahydrofolate to form L-glutamate and N^5-formimino-THF, or the formimino group may be hydrolyzed directly to formamide and L-glutamate. Alternatively, the formimino group may be deiminated to form ammonia and *N*-formyl-L-glutamate (HutF), which is subsequently hydrolyzed to formate and L-glutamate (HutG). These pathways are illustrated in Scheme 2. In this paper we report the cloning, expression, and characterization of Pa5106 from *P. aeruginosa*, along with two other proteins from this same organism, Pa5091 and Pa3175. We demonstrate that Pa5106 catalyzes the hydrolysis of *N*-formimino-L-glutamate to ammonia and *N*-formyl-L-glutamate, while Pa5091 catalyzes the hydrolysis

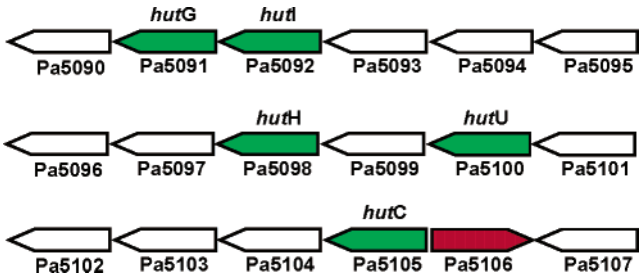

FIGURE 1: Genomic environment of the histidine degradation locus in *P. aeruginosa*. The relative lengths of the ORFs are not drawn to scale. The designation of the protein for each gene is provided, and the genes that code for production of HutG, HutI, HutH, HutU, and HutC are designated as such. The gene annotated as a probable chlorohydrolase is colored red (Pa5106).

Scheme 2: Pathways for Histidine Degradation

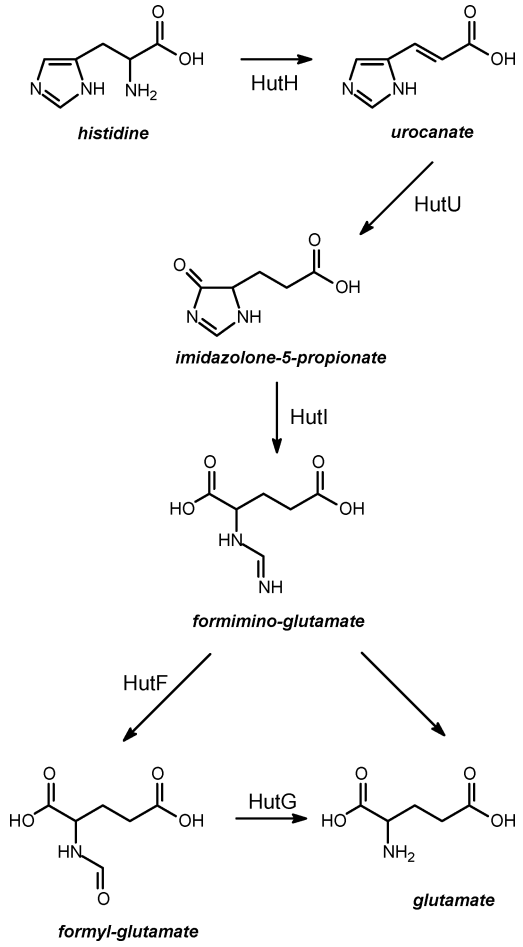

of *N*-formyl-L-glutamate to formate and L-glutamate. The protein Pa3175, which is dislocated from the Hut operon, is shown to catalyze the hydrolysis of *N*-formimino-L-glutamate to formamide and L-glutamate.

MATERIALS AND METHODS

Materials. All chemicals and coupling enzymes were obtained from Sigma or Aldrich, unless otherwise stated. The genomic DNA from *P. aeruginosa* was purchased from the American Type Culture Collection (ATCC). The oligonucleotide synthesis and DNA sequencing reactions were performed by the Gene Technology Laboratory of Texas A&M University. The pET30a(+) expression vector was acquired from Novagen. The T4 DNA ligase and the restriction enzymes, *Nde*I and *Hin*dIII, were purchased from New England Biolabs. The Platinum *Pfx* DNA polymerase and the Wizard Plus SV Mini-Prep DNA purification kit were obtained from Invitrogen and Promega, respectively.

Cloning and Site-Directed Mutagenesis. The genes encoding Pa5106, Pa5091, and Pa3175 from *P. aeruginosa* were amplified from the genomic DNA by standard PCR methods, stipulated in the manufacturer's instructions. The PCR primers contain *Nde*I and *Hin*dIII restriction sites at either end. The PCR products were purified, digested with *Nde*I and *Hin*dIII, ligated to the expression vector pET30a(+) using T4 DNA ligase, and then transformed into XL1Gold cells. Individual colonies containing the plasmid were selected on LB plates containing 50 μg/mL kanamycin and

then used to inoculate 5 mL cultures of LB. The entire coding region of the plasmids containing the genes for Pa5106, Pa5091, and Pa3175 were sequenced to confirm the fidelity of the PCR amplification.

Purification of Pa3175, Pa5091, and Pa5106. Cells harboring the plasmid for the expression of Pa5106 were grown overnight, and a single colony was used to inoculate 50 mL of LB media containing 50 μM kanamycin and subsequently used to inoculate 4 L of the same medium. Cell cultures were grown at 37 °C with a rotatory shaker until an A_{600} of ~0.6 was reached. Induction was initiated by the addition of 1.0 mM isopropyl-thiogalactoside (IPTG), and the cultures were further incubated overnight. The bacterial cells were isolated by centrifugation at 4500*g* for 15 min at 4 °C. The pellet was resuspended in 50 mM Hepes buffer, pH 7.5 (buffer A) containing 0.1 mg/mL of the protease inhibitor (PMSF) per gram of wet cells and then disrupted by sonication. The soluble fraction was separated from the lysed cells by centrifugation at 12000*g* for 15 min at 4 °C. Nucleic acids were precipitated by the addition of proteamine sulfate to a concentration of 1.5% (w/v). The soluble proteins were fractionated between 40% and 60% saturation of ammonium sulfate. The precipitated protein was resuspended in a minimum quantity of buffer A and loaded onto a High Load 26/60 Superdex 200 prep grade gel filtration column (Amersham Pharmacia) and eluted with buffer A. Fractions that contained Pa5106 were identified by SDS−PAGE, pooled and loaded onto a 6 mL Resource Q anion ion exchange column (Amersham Pharmacia) and eluted with a gradient of NaCl in 20 mM Hepes, pH 8.1 (buffer B). The fractions containing Pa5106 were pooled and reprecipitated by saturation with ammonium sulfate, centrifuged at 12000*g* for 15 min at 4 °C, and resuspended in a minimum amount of buffer A. The final step in the purification was accomplished by chromatography on a Superdex 200 column. The purity of the protein during the isolation procedure was monitored by SDS−PAGE. The purification of Pa3175 and Pa5091 was performed as described above with minimum modifications. In the case of Pa5091, buffer A was supplemented with 5 mM dithiothreitol (DTT) and the ammonium sulfate fractionation was accomplished between 20% and 60% of saturation. For Pa3175, the cell pellet was resuspended in buffer A supplemented with 50 μM $MnCl_2$ and 2.5 mM glutathione at pH 8.5.

Molecular Weight Determination. A HiLoad 16/60 Superdex 200 column (Pharmacia) was calibrated with six standard molecular weight markers (MW-GF-1000 from Sigma). Pa5106, Pa5091, and Pa3175 were applied to the column in sequential runs and eluted with buffer A at a flow rate of 1.0 mL per minute. The elution volume for each of the proteins was used to calculate the apparent molecular weight of the protein in solution.

Metal Analysis and Amino Acid Sequence Verification. The purified Pa5106 was subjected to N-terminal amino acid sequence analysis by the Protein Chemistry Laboratory at Texas A&M University. The first six amino acids were MSAIFA, which agrees with the reported protein sequence for Pa5106. The N-terminal amino acid sequence analysis for the first five amino acids of purified Pa5091 gave the sequence as MYPAPD, which corresponds to the reported protein sequence. In the case of Pa3175, the amino acid sequence obtained for the first six amino acids was MDEVLS, which matches the reported protein sequence.

The protein concentration was determined spectrophotometrically at 280 nm using a SPECTRAmax-340 microplate reader (Molecular Devices Inc.). The extinction coefficients used for these measurements were 66 810 M^{-1} cm^{-1} for Pa5106, 40 800 M^{-1} cm^{-1} for Pa5091, and 45 080 M^{-1} cm^{-1} for Pa3175 based upon the derived protein sequence. The metal content of the purified proteins was determined with a Perkin-Elmer AAnalyst 700 atomic absorption spectrometer and by inductively coupled plasma emission-mass spectrometry (ICP-MS). Pa5106 contained 1.2 equiv of Zn^{2+} per subunit, and Pa5091 contained 1.1 equiv of Zn^{2+}. The metal content of Pa3175 was found to be 0.2 equiv of Mn^{2+} and 0.4 equiv of Zn^{2+}. The metal was removed from Pa5106 by treating the protein with 3 mM dipicolinate at 4 °C at pH 5.6 for 48 h. The chelator was removed by loading the chelator/protein mixture onto a PD10 column (Amersham Biosciences) and eluting with metal-free buffer A. Metal-free buffer A was prepared by passage through a column of Chelex 100 resin. The apo-Pa5106 was reconstituted with the addition of 1 equiv of the desired metal (Zn^{2+}, Co^{2+}, Ni^{2+}, Cd^{2+}, and Mn^{2+}) in 50 mM HEPES at pH 7.5. The metal content of the reconstituted proteins was verified using a Perkin-Elmer AAnalyst 700 atomic absorption spectrometer and ICP-MS.

*Synthesis of N-Formimino-L-glutamate (**1**).* L-Glutamic acid (1.47 g, 10 mmol), formamidine hydrochloride (1.61 g, 20 mmol), silver carbonate (3.03 g, 11 mmol), and formamide (8 mL) were added to a 100 mL flask and stirred at room temperature for 36 h (*14*). After the reaction was complete, the excess ammonia and carbon dioxide were removed under reduced pressure for a period of 30 min. At this time, 150 mL of 0.06 N HCl was added and the pH was adjusted to between 4 and 6. The mixture was filtered and the carbon dioxide was removed under vacuum. The solution was applied to a column of Dowex-1-acetate, washed with water (150 mL), and then eluted with 0.5 M acetic acid. The *N*-formimino-L-glutamate was isolated with an overall yield of 40% (0.70 g). ^{1}H NMR (300 MHz, D_2O): 7.60 ppm (1H, s, C*H*═NH), 4.02 ppm (1H, t, J = 5.7 Hz, C*H*NH), 3.92 ppm, (1H, t, J = 5.7 Hz, C*H*NH), 2.26 ppm (2H, t, J = 7.2 Hz, CH_2CO), 2.12−1.89 ppm (2H, m, CHCH_2). ^{13}C NMR (75.4 MHz, D_2O): 177.43, 177.36, 175.66, 174.33, 157.14, 153.90, 60.58, 55.38, 30.30, 30.08, 27.65, and 26.14 ppm. Mass spectrometry (ESI negative mode): observed, 173.03 $(M - H)^-$; expected, 173.06 $(M - H)^-$. The rest of the *N*-formimino amino acid derivatives were synthesized using a similar protocol, and the relevant spectroscopic data are presented in the Supporting Information.

*Synthesis of N-Formyl-L-glutamate (**2**).* Acetic anhydride (8 mL) was added dropwise to a 100 mL flask containing L-glutamic acid (4.41 g, 30 mmol) and formic acid (50 mL) (*15*). After stirring for 30 min, the reaction was stopped by the addition of 2 mL of water and the solvent removed by rotary evaporation. The compound was purified by chromatography on a silica gel column using a 6/1 mixture of chloroform and methanol (v/v) as the eluant. The solvent was removed and the solid material washed with ethyl acetate and ether and then dried to obtain 2.11 g of material with an overall yield of 40%. ^{1}H NMR (300 MHz, DMSO): 12.42 ppm (1H, s, COO*H*), 8.37 ppm (1H, d, J = 7.2 Hz, N*H*),

8.03 ppm (1H, s, C*H*O), 4.32−4.24 ppm (1H, m, C*H*NH), 2.28−2.23 ppm (2H, m, $CHCH_2CH_2$), 2.02−1.91 ppm (1H, m, $CHCH_2CH_2$), 1.83−1.68 ppm (1H, m, $CHCH_2CH_2$). Mass spectrometry (ESI negative mode): observed, 174.2 $(M - H)^-$; expected, 174.05 $(M - H)^-$. The rest of the *N*-formyl amino acid derivatives were synthesized using a similar protocol, and the relevant spectroscopic data are presented in the Supporting Information.

Assay for Deimination of N-Formimino Amino Acids. The measurement of the enzymatic activity for the deimination of *N*-formimino amino acids was conducted by coupling the production of ammonia to the oxidation of NADH with glutamate dehydrogenase. The decrease in the concentration of NADH was followed spectrophotometrically at 340 nm using a SPECTRAmax-340 microplate reader (Molecular Devices Inc.). The standard assay was modified from the report by Muszbek et al. (*16*) and contained 100 mM Hepes at pH 8.0, 100 mM KCl, 7.4 mM α-ketoglutarate, 0.4 mM NADH, 6 units of glutamate dehydrogenase, and the appropriate *N*-formimino amino acid in a final volume of 250 μL at 30 °C. The following compounds were tested for enzymatic activity at a concentration of 10 mM using this protocol: *N*-formimino-L-glutamate (**1**), *N*-formimino-D-glutamate (**8**), *N*-guanidino-L-glutamate (**5**), *N*-formimino-α-aminobutyric acid (**6**), *N*-formimino-γ-aminobutyric acid (**7**), *N*-formimino-L-alanine, *N*-formimino-L-aspartate (**9**), *N*-formimino-glycine, *N*-formimino-L-isoleucine, *N*-formimino-L-leucine, *N*-formimino-L-methionine, *N*-formimino-L-phenylalanine, *N*-formimino-L-tyrosine, and *N*-formimino-L-valine.

Assay for Hydrolysis of N-Formyl Amino Acids. The enzymatic deformylation of *N*-formyl amino acids was monitored by following the production of formate with formate dehydrogenase. The increase in the concentration of NADH was measured spectrophotometrically at 340 nm using a SPECTRAmax-340 microplate spectrophotometer. The protocol was modified from the reported assay of Nanba et al. (*17*) and contained 100 mM Hepes at a pH of 7.5, 100 mM KCl, 5 mM DTT, 5 mM NAD^+, and the appropriate amount of an *N*-formyl amino acid in a final volume of 250 μL at 30 °C. The following *N*-formyl amino acids were tested as substrates for this activity at a concentration up to 10 mM: *N*-formyl-L-glutamate (**2**), *N*-formyl-D-glutamate, *N*-formyl-L-alanine, *N*-formyl-L-aspartate, *N*-formyl-glycine, *N*-formyl-L-isoleucine, *N*-formyl-L-leucine, *N*-formyl-L-methionine, *N*-formyl-L-phenylalanine, *N*-formyl-L-tyrosine, and *N*-formyl-L-valine.

Assay for Hydrolysis of N-Acyl Amino Acids. The enzymatic hydrolysis of *N*-acyl L-glutamic acids was followed by coupling the production of L-glutamate to the reduction of NAD^+ by glutamate dehydrogenase and the subsequent transformation of iodonitrotetrazolium (INT) to INT-formazan by diaphorase. The formation of INT-formazan was monitored at 500 nm. The standard assay was modified from the protocol of Beutler (*18*) and contained 100 mM Hepes at pH of 8.5, 1.5 mM NAD^+, 1.5 mM *p*-iodonitrotetrazolium violet, 2.0 units of diaphorase, 6 units of glutamate dehydrogenase, and the appropriate amount of the *N*-acyl L-glutamic amino acid in a final volume of 250 μL at 30 °C. Several *N*-acyl amino acids were tested for activity with this assay: *N*-formimino-L-glutamate (**1**), *N*-guanidino-L-glutamate (**5**), *N*-carbamoyl-L-glutamate (**4**), *N*-acetyl-L-glutamate (**3**), and *N*-formyl-L-glutamate (**2**). The assay described above was modified to monitor the formation of L-alanine by substitution of 7 units of alanine dehydrogenase for glutamate dehydrogenase. The following compounds were assayed for the formation of L-alanine at a concentration of 10 mM: *N*-formimino-L-alanine, *N*-carbamoyl-L-alanine, *N*-acetyl-L-alanine, and *N*-formyl-L-alanine.

The hydrolysis of *N*-acyl L-aspartic acid derivatives was monitored by following the production of aspartate spectrophotometrically at 340 nm using the combined enzymatic activities of malate dehydrogenase and aspartate aminotransferase. The standard assay contained 100 mM Hepes (pH 8.1), 100 mM KCl, 3.7 mM α-ketoglutarate, 0.4 mM NADH, 0.64 unit of malate dehydrogenase, 6 units of aspartate aminotransferase, and the *N*-acyl-L-aspartate derivative in a final volume of 250 μL at 30 °C. The following compounds were tested for enzymatic activity at a concentration of 10 mM: *N*-formimino-L-aspartate (**9**), *N*-carbamoyl-L-aspartate, *N*-acetyl-L-aspartate, and *N*-formyl-L-aspartate.

Inhibition of Pa5106 by N-Acyl-L-glutamate Analogues: The inhibition of the enzymatic deimination of *N*-formimino-L-glutamate (**1**) by Pa5106 was studied. *N*-acetyl-L-glutamate (**3**), *N*-carbamoyl-L-glutamate (**4**), *N*-formimino-L-aspartate (**9**), *N*-formimino-α-aminobutyric acid (**6**), *N*-formimino-γ-aminobutyric acid (**7**), *N*-formyl-L-glutamate (**2**), *N*-guanidino-L-glutamate (**5**), and *N*-succinyl-L-glutamate were tested as inhibitors using the assay that monitors formation of ammonia with *N*-formimino-L-glutamate (**1**) as the substrate.

Data Analysis. The kinetic parameters, k_{cat} and k_{cat}/K_m, were determined by fitting the initial velocity data to eq 1, where v is the initial velocity, E_t is the enzyme concentration, k_{cat} is the turnover number, A is the substrate concentration, and K_m is the Michaelis constant (*19*). Competitive inhibition patterns were fitted to eq 2, where I is the inhibitor concentration and K_i is the inhibition constant (*19*).

$$v/E_t = k_{cat}A/(K_m + A) \quad (1)$$

$$v/E_t = k_{cat}A/(K_m((1 + I)/K_i) + A) \quad (2)$$

RESULTS

Purification and Properties of Pa5106. The protein Pa5106 was produced in high quantities after the modified pET30a-(+) plasmid was transformed in BL21(DE3)star cells. The protein was purified to homogeneity and found to contain 1.2 equiv of Zn^{2+} per subunit. SDS−PAGE analysis of the isolated protein gave a single band which corresponds to an apparent molecular weight of 49 kDa, which agrees with the reported gene sequence. The molecular weight of the native protein was found to be 100 kDa when measured from the elution volume of a calibrated gel filtration column, and thus Pa5106 is a dimer in solution.

The localization of the gene that encodes the protein sequence for Pa5106 suggests that this enzyme is likely involved in the metabolism of *N*-formimino-L-glutamate. The reaction catalyzed by Pa5106 was determined by NMR spectroscopy. When *N*-formimino-L-glutamate (**1**) was incubated with the enzyme at pH 8.0, the proton resonances for the hydrogen attached to the carbon of the formimino group (7.68 and 7.66 ppm) disappeared and were replaced by two new resonances at 7.95 and 7.81 ppm. These new resonances are coincident with the proton attached to the

Table 1: Kinetic Parameters for Metal-Reconstituted Forms of Pa5106[a]

HutF	K_m (mM)	k_{cat} (s^{-1})	k_{cat}/K_m (M^{-1} s^{-1})
WT (Zn)	0.22 ± 0.03	13.2 ± 0.4	(6.0 ± 0.8) × 10^4
WT (Ni)	2.7 ± 0.1	21.3 ± 0.3	(8.0 ± 0.3) × 10^3
WT (Cd)	2.1 ± 0.3	31.0 ± 0.1	(1.5 ± 0.2) × 10^4
WT (Cu)	1.2 ± 0.1	8.5 ± 0.1	(7.3 ± 0.6) × 10^3

[a] The kinetic parameters were determined with *N*-formimino-L-glutamate as the substrate at pH 8.0, 30 °C from a fit of the data to eq 1.

formyl group of *N*-formyl-L-glutamate, and thus Pa5106 catalyzes the deamination of *N*-formimino-L-glutamate to ammonia and *N*-formyl-L-glutamate. The rate of this reaction was subsequently measured by monitoring the formation of ammonia with glutamate dehydrogenase. The turnover number of the purified protein for the deimination of *N*-formimino-L-glutamate (**1**) is 13 s^{-1} at pH 8.0, and the Michaelis constant is 220 μM.

The requirement of the single zinc ion bound to the protein was determined by the preparation of the apo-enzyme via the removal of the metal with chelators. The specific activity of apo-Pa5106 was less than 1% of the holo-enzyme. The metal center in the apo-enzyme was reconstituted with 1 equiv of the other divalent cations in approximately 10 min. The reconstitution of apo-Pa5106 resulted in catalytically active enzyme in the presence of Cd^{2+}, Ni^{2+}, Zn^{2+}, or Cu^{2+}. The reconstitution of apo-Pa5106 with Co^{2+} or Mn^{2+} was not successful under the conditions used for this investigation. The kinetic parameters for the metal reconstituted forms of Pa5106 are presented in Table 1.

Substrate Specificity of Pa5106. A variety of compounds were tested as potential substrates for Pa5106. *N*-Formimino-L-glutamate (**1**) was found to be the best substrate with a K_m of 0.22 mM and a k_{cat} of 13 s^{-1}. The catalytic activity of *N*-formimino-D-glutamate (**8**) was less than or equal to 5.0 × 10^{-2} s^{-1} at a concentration of 10 mM. At a concentration of 10 mM, *N*-formimino-L-isoleucine and *N*-formimino-L-methionine were turned over with rate constants that were less than or equal to 1.9 × 10^{-2} s^{-1} and 1.0 × 10^{-2} s^{-1}, respectively. The remaining *N*-formimino-L-amino acids and other *N*-acyl substituted forms of glutamate tested as substrates for this enzyme were all found to be turned over with specific activities less than 1.0 × 10^{-3} s^{-1} under these conditions. The compounds tested were the following: *N*-formimino-L-alanine, *N*-formimino-L-aspartate (**9**), *N*-formimino-glycine, *N*-formimino-L-isoleucine, *N*-formimino-L-leucine, *N*-formimino-L-methionine, *N*-formimino-L-phenylalanine, *N*-formimino-L-tyrosine, *N*-formimino-L-valine, *N*-guanidino-L-glutamate, *N*-formimino-α-aminobutyric acid (**6**), *N*-formimino-γ-aminobutyric acid (**7**), *N*-acetyl-L-glutamate (**3**), *N*-carbamoyl-L-glutamate (**4**), and *N*-formyl-L-glutamate (**2**). The structures for some of these compounds are presented in Scheme 3. These results demonstrate that Pa5106 from *P. aeruginosa* is an *N*-formimino-L-glutamate deiminase.

Inhibition of Pa5106 by N-Acyl L-Glutamate Analogues. The compounds *N*-acetyl-L-glutamate (**3**), *N*-carbamoyl-L-glutamate (**4**), *N*-formimino-L-aspartate (**9**), *N*-formimino-α-aminobutyric acid (**6**), *N*-formimino-γ-aminobutyric acid (**7**), *N*-formyl-L-glutamate (**2**), *N*-guanidino-L--L-glutamate (**5**), and *N*-succinyl-L-glutamate were tested as inhibitors for the deimination of *N*-formimino-L-glutamate (**1**) by Pa5106. No inhibition could be detected from *N*-acetyl-L-glutamate (**3**), *N*-carbamoyl-L-glutamate (**4**), and *N*-formyl-L-glutamate (**2**) at concentrations up to 10 mM. The substrate analogues that lack the carboxylate group at the α or γ positions (*N*-formimino-α-aminobutyric acid (**6**) and *N*-formimino-γ-aminobutyric acid (**7**)), did not inhibit the reaction at concentrations up to 10 mM. *N*-Guanidino-L-glutamate (**5**) and *N*-formimino-L-aspartate (**9**) were competitive inhibitors with K_i values of 890 μM and 30 μM, respectively.

Scheme 3: Structures of Selected Substrates and Inhibitors Utilized in This Investigation

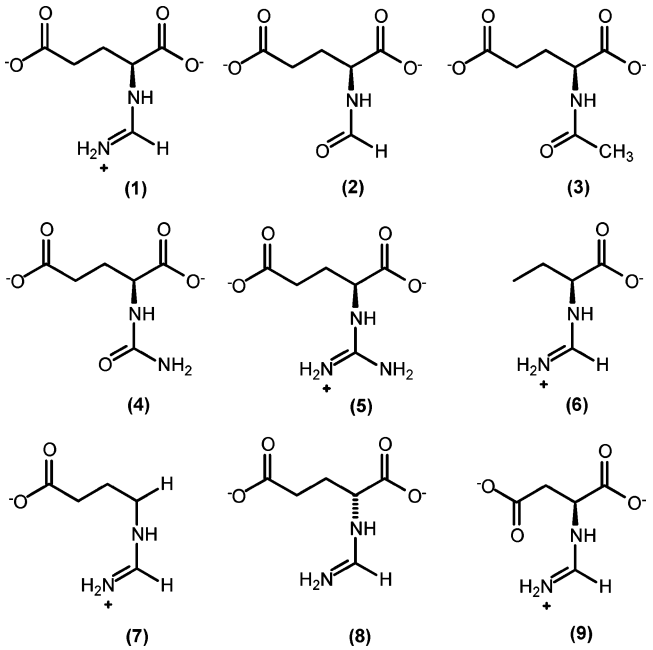

Purification and Properties of Pa5091. The protein Pa5091 was overexpressed when the appropriate plasmid was transformed in BL21(DE3)star cells. The protein was isolated by standard methods and purified to greater than 95% as judged by SDS−PAGE with an apparent molecular weight of 30 kDa. The predicted size of the protein is 29 824 Da based upon the DNA sequence. The molecular weight of the protein, determined from the elution volume of a calibrated gel filtration column, was 28 kDa, and thus Pa5091 is a monomer in solution. The purified protein was found to contain 1.1 equiv of Zn^{2+} per subunit.

The original expectation for Pa5091 was that this protein would catalyze the hydrolysis of *N*-formyl-L-glutamate to formate and L-glutamate. When Pa5091 was incubated with *N*-formyl-L-glutamate, the NMR resonance at 7.95 ppm for the hydrogen attached to the formyl group disappeared and was replaced by a new resonance at 8.32 ppm. The resonance at 8.32 ppm is identical to that found for formate. The formation of formate was confirmed and quantified by monitoring the reaction spectrophotometrically with formate dehydrogenase.

Substrate Specificity of Pa5091. Several N-substituted amino acids were tested for catalytic activity with Pa5091. These compounds included *N*-formyl-L-alanine, *N*-formyl-L-aspartate, *N*-formyl-D-glutamate, *N*-formyl-L-glutamate, *N*-formyl-L-glutamine (**2**), *N*-formyl-glycine, *N*-formyl-L-isoleucine, *N*-formyl-L-leucine, *N*-formyl-L-methionine, *N*-formyl-L-phenylalanine, *N*-formyl-L-tyrosine, *N*-formyl-L-

valine, *N*-acetyl-L-glutamate (**3**), *N*-carbamoyl-L-glutamate (**4**), and *N*-formimino-L-glutamate (**1**). From these compounds only *N*-formyl-L-glutamate (**2**) and *N*-formyl-L-glutamine exhibited any detectable activity with Pa5091. The hydrolysis of the formyl group from *N*-formyl-L-glutamate by Pa5091 proceeded with a k_{cat} of 1.01 ± 0.04 s^{-1} and a K_m of 3.3 ± 0.4 mM at pH 7.5. The value for k_{cat}/K_m is 306 ± 40 M^{-1} s^{-1}. In the case of *N*-formyl-L-glutamine, saturation could not be achieved within the solubility limits of this compound. The value for k_{cat}/K_m was found to be 14.9 ± 0.5 M^{-1} s^{-1}. At a concentration of 10 mM, the upper limit for the turnover number for the hydrolysis of *N*-formyl-L-lysine, *N*-formyl-L-histidine, and *N*-formyl-L-arginine was 2.6 × 10^{-2} s^{-1}. All other compounds tested showed specific activities less than 1.0 × 10^{-3} s^{-1} at a concentration of 10 mM. These results demonstrate that Pa5091 from *P. aeruginosa* is *N*-formyl-L-glutamate deformylase.

Purification and Properties of Pa3175. The protein Pa3175 was readily purified following overexpression of the protein in *Escherichia coli* from the modified vector pET30a(+). The purified protein migrated as a single band on SDS−PAGE with an apparent molecular weight of 34 kDa. The theoretical molecular weight based on the DNA sequence is 34 230 Da. On a calibrated gel filtration column Pa3175 migrated with a molecular weight of 69 kDa, and thus this protein is a dimer in solution. The purified protein had 0.2 equiv of Mn^{2+} and 0.4 equiv of Zn^{2+} per subunit. This protein was shown to catalyze the hydrolysis of *N*-formimino-L-glutamate (**1**) to formamide and L-glutamate. This was confirmed by the appearance of a new proton resonance at 7.93 ppm that is identical to formamide using NMR spectroscopy. The formation of L-glutamate was confirmed spectrophotometrically using glutamate dehydrogenase.

Substrate Specificity of Pa3175. The compounds *N*-formimino-L-glutamate (**1**), *N*-acetyl-L-glutamate (**3**), *N*-carbamoyl-L-glutamate (**4**), *N*-formyl-L-glutamate (**2**), *N*-formimino-L-aspartate (**9**), *N*-acetyl-L-aspartate, *N*-formyl-L-aspartate, *N*-formimino-L-alanine, *N*-acetyl-L-alanine, and *N*-formyl-L-alanine were tested as potential substrates for Pa3175. The sole compound to show activity was *N*-formimino-L-glutamate (**1**) with a k_{cat} of 73 ± 4 s^{-1} and a K_m of 4.3 ± 0.6 mM. The value of k_{cat}/K_m was (1.72 + 0.03) × 10^4 M^{-1} s^{-1}. All of the other compounds tested failed to shown any turnover with specific activities less than 1.0 × 10^{-3} s^{-1}. These results establish that Pa3175 catalyzes the hydrolysis of *N*-formimino-L-glutamate to L-glutamate and formamide.

DISCUSSION

Enzymes belonging to the amidohydrolase superfamily are found in every organism sequenced to date. Well over 1000 gene sequences have been identified as members of this superfamily among the first 200 completely sequenced bacterial genomes. Enzymes within this protein superfamily catalyze primarily the hydrolysis of C−N or P−O bonds in amino acids, carbohydrates, and nucleic acids. Within the genome of *Escherichia coli* K12 there are 18 members of this superfamily. Eleven of these enzymes catalyze known chemical transformations while the substrates for the remaining seven enzymes have not, as yet, been identified. Thus, the substrate and reaction diversity for a significant fraction of the amidohydrolase superfamily is unknown. Many of the homologous subgroups within the amidohydrolase superfamily of unknown or ambiguous function have been annotated as probable chlorohydrolases or cytosine deaminase-like. One of these subgroups that share an overall sequence identity of 40% to one another is presented in the dendrogram that appears in Figure 2. Within this subgroup of 39 sequences is the protein Pa5106 from *P. aeruginosa*. An inspection of the location of these genes within the context of the genomes in which they reside demonstrates that in each case they are localized adjacent to other genes that are involved in the degradation of histidine. This observation suggests that Pa5106 may be part of the operon that is responsible for the catabolism of the amino acid histidine. The complete sequence alignment for the 39 sequences that are analogues to Pa5106 is provided in the Supporting Information.

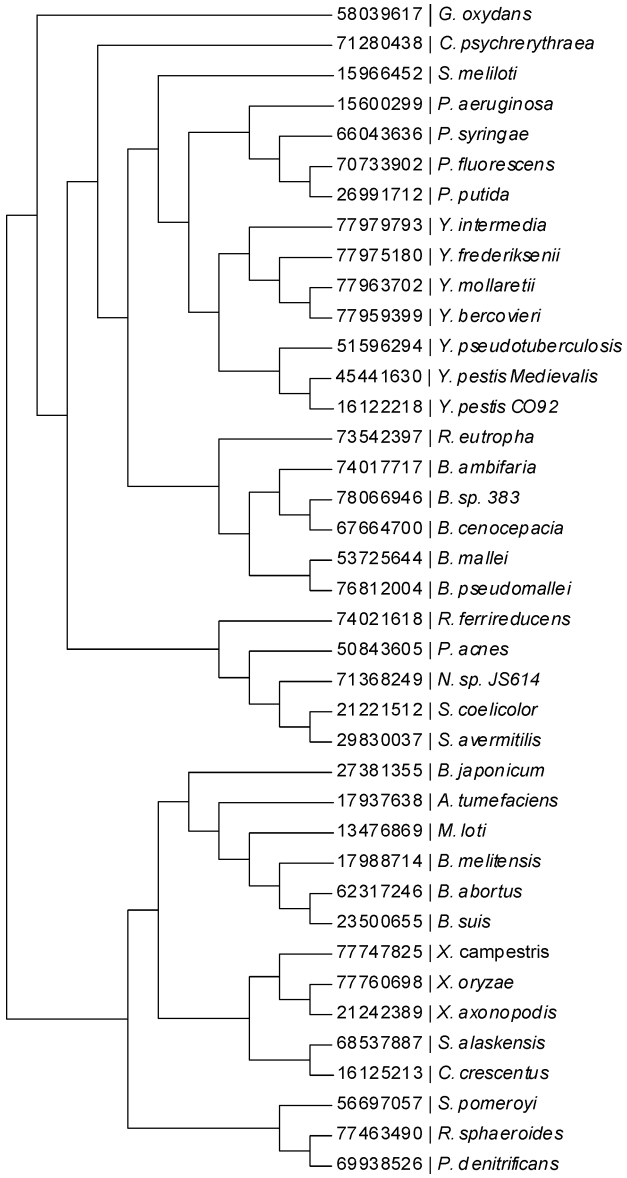

FIGURE 2: Dendrogram of microbial HutF homologues. HutF can be divided into 2 major groups with a cutoff of 40% identity. The *Actinomycetales* species, *P. acnes*, *S. avermitilis*, *S. coelicolor*, and *N. sp*. JS614, form the smaller group. The members of the smaller group are 30−39% identical to sequences in the larger group.

```
Pa5106  ----------MSAIFAERALLPEGWARNVRFEISADGVLAEIRPD-ANAD 39
AtzA    MQTLSIQHGTLVTMDQYRRVLGDSWVHVQDGRIVALG-VHAESVPPPADR 49
Tm0936  ---MIIGNCLILKDFS--SEPFWGAVEIENGTIKRVL-------QGEVKV 38

Pa5106  GAERLGGAVLPGMPNLHSHAFQRAMAGLAEVAGNPNDSFWTWRELMYRMV 89
AtzA    VIDARGKVVLPGFINAHTHVNQILLRGGPSHGRQFYD--WLFNVVYPGQK 97
Tm0936  DLDLSGKLVMPALFNTHTHAPMTLLR-GVAEDLSFEE--WLFSKVLPIED 85

Pa5106  ARLSPEQIEVIACQLYIEMLKAGYTAVAEFHYVHHDLDGRSY-------- 131
AtzA    AMR-PEDVAVAVRLYCAEAVRSGITTINENADSAIYPGNIEAAMAVYGEV 146
Tm0936  RLT-EKMAYYGTILAQMEMARHGIAGFVD-------------------- 113

Pa5106  ADPAELSLRISRAASAAGIGLTLLPVLYSHAGFGGQPASEGQRRFINGSE 181
AtzA    GVRVVYARMFFDRMDGRIQGYVDALKARSPQVELCSIMEETAVAKDRITA 196
Tm0936  -------MYFHEEWIAKAVRDFGMRALLTRGLVDSNGDDG--GRLEENLK 154

Pa5106  AYLELLQRLRAPLEAAGHSLGLCFHSLRAVTPQQIATVLA---AGHDDLP 228
AtzA    LSDQYHGTAGGRIS-----VWPAPATTTAVTVEGMRWAQAFAR--DRAVM 239
Tm0936  LYNEWNG-FEGRIF-----VGFGPHSPYLCSEEYLKRVFDTAK--SLNAP 196

Pa5106  VHIHIAEQQKEVDDCQAWSGRRPLQWLYENVAVDQRWCLVHATHADPAEV 278
AtzA    WTLHMAESDHDER----IHGMSPAEYMECYGLLDERLQVAHCVYFDRKDV 285
Tm0936  VTIHLYETSKEEYDLED---------ILNIGLKEVKTIAAHCVHLPERYF 237

Pa5106  AAMARSGAVAGLCLSTEANLGDGIFPATDFLAQGGRLGIGSDSHVSLSVV 328
AtzA    RLLHRHNVKVASQVVSNAYLGSGVAPVPEMVERGMAVGIGTDNGNSNDSV 335
Tm0936  GVLKDIPFFVSHNPASNLKLGNGIAPVQRMIEHGMKVTLGTDGAASNNSL 287

Pa5106  EELRWLEYGQRLRDRKR-NRLYRDDQPMIGRTLYDAALAGGAQALGQPIG 377
AtzA    NMIGDMKFMAHIHRAVHRDADVLT-----PEKILEMATIDGARSLGMDHE 380
Tm0936  NLFFEMRLASLLQKAQ--NPRNLD-----VNTCLKMVTYDGAQAMG--FK 328

Pa5106  S--LAVGRRADLLVLDGNDPYLASAEGDALLNRWLFAG-GDRQVRDVMVA 424
AtzA    IGSIETGKRADLILLDLRHPQTTPHHH---LAATIVFQAYGNEVDTVLID 427
Tm0936  SGKIEEGWNADLVVIDLDLPEMFPVQN---IKNHLVHAFSG-EVFATMVA 374

Pa5106  GRWVVRDG-RHAGE-ERSA---RAFVQVLGELLD------------- 453
AtzA    GNVVMENRRLSFLPPERELAFLEEAQSRATAILQRANMVANPAWRSL 474
Tm0936  GKWIYFDGEYPTID---SEEVKRELARIEKELYSS------------ 406
```

FIGURE 3: Alignment of Pa5106 and AtzA to the structure, 1p1m (Tm0936). The metal ligands are indicated in bold type. The conserved glutamate after strand 5 is indicated by a box. The beta strands of the alpha beta barrel are highlighted. The residues which interact with the substrate are either immediately after the strands or in the loops which connect the strands to the following alpha helix. With the exception of Tm0936, for which there is a structure, the strands are predicted based on alignment, homology, secondary structure prediction, and presence of turn forming residues such as glycine and proline. The alignment was done with ClustalX using the sequences within 40% identity of each sequence shown.

The chemical transformations for the degradation of histidine are presented in Scheme 2, and the genes for four of these enzymes are clearly identified within the genome of *P. aeruginosa*: histidine ammonia lyase (HutH; Pa5098), urocanase (HutU; Pa5100), imidazolone propionate amidohydrolase (HutI; Pa5092), and *N*-formyl-L-glutamate deformylase (HutG; Pa5091). This observation indicates that the degradation of histidine in *P. aeruginosa* follows the same path as previously reported for *Pseudomonas fluorescens* (*15*) and *Pseudomonas putida* (*20*) if the enzyme responsible for the deimination of *N*-formimino-L-glutamate can be identified. We have now demonstrated that the missing enzyme within this pathway is Pa5106. It is also highly likely that the 38 other sequences that are also found adjacent to the hut operon in other organisms should now be annotated as *N*-formimino-L-glutamate deiminase. The gene for this enzyme has sometimes been labeled as *hut*F.

The substrate specificity for Pa5106 is rather narrow. A total of 14 *N*-formimino amino acids were tested as substrates, but only *N*-formimino-L-glutamate was found to be hydrolyzed at a significant rate. No turnover could be detected with the D-enantiomer, and no activity could be detected when either of the two carboxylate groups from the glutamate moiety were deleted. In addition, the enzyme was unable to hydrolyze other substituents attached to the α-amino group of L-glutamate, including guanidino, formyl, acetyl, and carbamoyl functional groups. The only two compounds that were significant competitive inhibitors of this enzyme were *N*-guanidino-L-glutamate (**5**) and *N*-formimino-L-aspartate (**9**).

An amino sequence alignment of Pa5106 with Tm0936 from *Thermotoga maritima* and atrazine chlorohydrolase (AtzA) from *Pseudomonas sp.* is shown in Figure 3. Since the X-ray crystal structure of Tm0936 (pdb: P1M1 and 1J6P) has been determined to high resolution, the residues that are expected to be within the active site of Pa5106 can be determined with a high degree of confidence from this alignment. Tm0936 folds as an $(\alpha/\beta)_8$-barrel, and the single divalent cation in the active site is ligated to two histidines found at the end of strand 1, a histidine at the end of strand five, and an aspartate at the end of strand 8. For Pa5106, these residues correspond to His-56, His-58, His-232, and

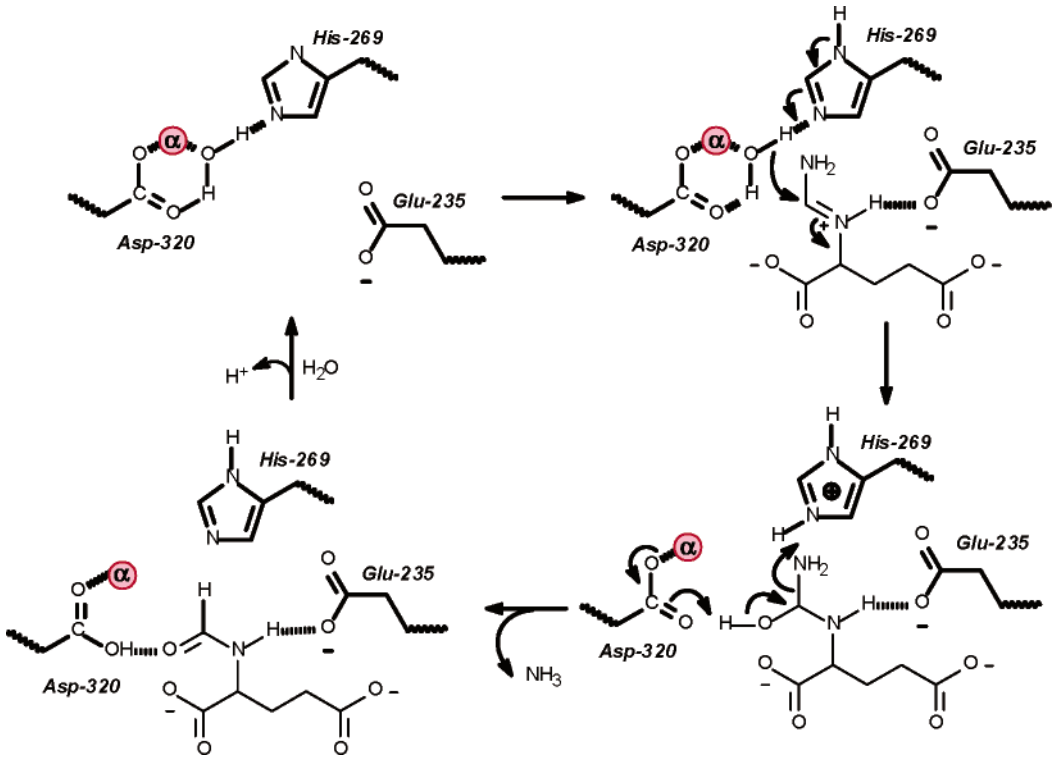

FIGURE 4: Working model for the chemical mechanism for the hydrolysis of *N*-formimino-L-glutamate by Pa5106. The red circle labeled α is used to indicate the divalent cation bound to the α-position within the active site (*10*).

Asp-320. The remaining highly conserved residue within this subfamily of amidohydrolase enzymes is a glutamate found three residues beyond the conserved histidine at the end of strand 5 (HxxE motif) (*21*−*23*). This glutamate has been postulated in cytosine and adenosine deaminase to serve as a general acid/base catalyst for proton transfer to the ring nitrogen during deamination (*21*−*23*). In Pa5106 this residue corresponds to Glu-235. The overall sequence identity of Pa5106 to Tm0936 and atrazine chlorohydrolase is 21% and 20%, respectively.

There appear to be two competing pathways for the degradation of *N*-formimino-L-glutamate (**1**) in *P. aeruginosa*. The protein Pa5091 is found within the Hut operon and has now been shown to catalyze the hydrolysis of *N*-formyl-L-glutamate (HutG). Together, Pa5106 and Pa5091 enable the two-step degradation of *N*-formimino-L-glutamate to ammonia, formate, and L-glutamate. The protein Pa5091 possesses a high specificity toward the hydrolysis of *N*-formyl-L-glutamate (**2**). Of fifteen compounds tested for activity, only *N*-formyl-L-glutamate and *N*-formyl-L-glutamine were hydrolyzed. The alternative pathway for histidine degradation is the direct hydrolysis of the formimino functional group of *N*-formimino-L-glutamate (**1**) to produce formamide and L-glutamate. The protein Pa3175 was purified and found able to catalyze the direct hydrolysis of the formimino group of *N*-formimino-L-glutamate. An array of *N*-acyl L-amino acid derivatives were tested for catalytic activity with this enzyme, but only *N*-formimino-L-glutamate was found to be a substrate. The reason for the existence of two different pathways for the degradation of *N*-formimino-L-glutamate (**1**) in *P. aeruginosa* is unclear. The proximity of the genes encoding for Pa5091 and Pa5106 to the Hut operon suggests that the degradation of L-histidine in *P. aeruginosa* takes place by the formation and hydrolysis of the *N*-formyl-L-glutamate intermediate.

The conservation of amino acids within the active site of Pa5106 with those of adenosine and cytosine deaminase enables a chemical reaction mechanism to be proposed for the deimination of *N*-formimino-L-glutamate. It was originally anticipated that Pa5106 would be responsible for the deamination of an aromatic base. This assumption was based on the observation that the conserved HxxE motif from the end of strand 5 in the amidohydrolase superfamily was found in enzymes such as adenosine deaminase, cytosine deaminase, AMP deaminase, and guanine deaminase (*21*, *23*). However, the formimino group is a rather nice mimic of the exocyclic amino group found in adenosine, cytosine, and guanine (see Scheme 1) and an analogous chemical mechanism can be proposed for Pa5106 based upon the mechanisms previously postulated for adenosine and cytosine deaminase.

A working model for the reaction mechanism catalyzed by Pa5106 is presented in Figure 4. In this mechanism the lone divalent cation is ligated to His-56, His-58, His-232, and Asp-320. The fifth ligand to the zinc is a water molecule from solvent that is also hydrogen bonded to His-269 and Asp-320. The substrate, *N*-formimino-L-glutamate, binds to this complex and initiates the abstraction of a proton from the bound water by His-269 and nucleophilic attack at the formimino carbon with the formation of a tetrahedral intermediate. The collapse of the tetrahedral intermediate is facilitated by proton transfer to Asp-320 and proton donation to the terminal amino substituent of the formimino group by the imidazolium group of His-269. The carbon−nitrogen bond is broken to generate ammonia and *N*-formyl-L-glutamate. The products dissociate and the active site is

regenerated by the binding of a molecule of water from solvent. Alternative reaction mechanisms can also be proposed depending on the ionization states of the three conserved residues in the active site (His-269, Glu-235, and Asp-320) and the tautomeric form of the substrate that initially binds to the active site. Experiments are in progress to discriminate among these alternative possibilities.

In this investigation, we have explored the final part of the histidine degradation pathway in *P. aeruginosa*. We have demonstrated the existence of an *N*-formimino-L-glutamate deiminase (Pa5106, HutF) as a member of the amidohydrolase superfamily and have confirmed the presence of *N*-formyl-L-glutamate deformylase (Pa5091, HutG). These two enzymes act in concert to catalyze the degradation of *N*-formimino-L-glutamate (**1**) to ammonia, formate, and L-glutamate. Substantially dislocated from these two genes in the Hut operon is a gene for the expression of protein Pa3175 which we have shown to catalyze the hydrolysis of *N*-formimino-L-glutamate (**1**) to formamide and L-glutamate. Both of the enzymes that act on *N*-formimino-L-glutamate possessed a high specificity with values of k_{cat}/K_m of 6.0×10^4 M^{-1} s^{-1} for Pa5106 and 1.7×10^4 M^{-1} s^{-1} for Pa3175. Due to the proximity of the genes encoding for Pa5106 (HutF) and Pa5091 (HutG) to the rest of the Hut operon, it is suggested that the degradation of L-histidine to L-glutamate in *P. aeruginosa* proceeds through the pathway that includes HutH, HutU, HutI, HutF, and HutG. A functional explanation for the existence of a formiminoglutaminase (Pa3175) is unknown.

ACKNOWLEDGMENT

We thank LaKenya Williams for the measurement of the NMR spectra for the products of the reaction catalyzed by Pa5106, Pa5091, and Pa3175.

SUPPORTING INFORMATION AVAILABLE

Information regarding the synthesis of *N*-acyl amino acids, and a complete amino acid sequence alignment for the other proteins identified as catalyzing the hydrolysis of *N*-formimino-L-glutamate. This material is available free of charge via the Internet at http://pubs.acs.org.

REFERENCES

1. Gerlt, J. A., and Babbitt, P. C. (2001) Divergent evolution of enzymatic function: Mechanistically diverse superfamilies and functionally distinct suprafamilies, *Annu. Rev. Biochem. 70*, 209−246.
2. Wise, E. L., and Rayment, I. (2004) Understanding the importance of protein structure to nature's routes for divergent evolution in TIM barrel enzymes, *Acc. Chem. Res. 37*, 149−158.
3. Gerlt, J. A., and Babbitt, P. C. (1998) Mechanistically diverse enzyme superfamilies: the importance of chemistry in the evolution of catalysis, *Curr. Opin. Chem. Biol. 2*, 607−612.
4. Holm, L., and Sander, C. (1997) An evolutionary treasure: Unification of a broad set of amidohydrolases related to urease, *Proteins 28*, 72−82.
5. Yang, Z., Savchenko, A., Yakunin, A., Zhang, R., Edwards, A., Arrowsmith, C., and Tong, L. (2003) Aspartate dehydrogenase, a novel enzyme identified from structural and functional studies of Tm1643, *J. Biol. Chem. 278*, 8804−8808.
6. Akita, M., Kayatama, K., Hatada, Y., Ito, S., and Horikoshi, K. (2005) A novel beta-glucanase gene from *Bacillus halodurans* C-125, *FEMS Microbiol. Lett. 248*, 9−15.
7. Thoden, J. B., Taylor Ringia, E. A., Garrett, J. B., Gerlt, J. A., Holden, H. M., and Rayment, I. (2004) Evolution of enzymatic activity in the enolase superfamily: structural studies of the promiscuous o-succinylbenzoate synthase from *Amycolatopsis*, *Biochemistry 43*, 5716−5727.
8. Wang, Z., Wei, H., Yu, Y., Sun, J., Yang, Y., Xing, G., Wu, S., Zhou, Y., Zhu, Y., Zhang, C., Zhou, T., Zhao, X., Sun, Q., and Hea, Z. (2004) Characterization of Ceap-11 and Ceap-16, two novel splicing variant proteins, associated with centrosome, microtubule aggregation and cell proliferation, *J. Mol. Biol. 343*, 71−82.
9. Roodveldt, C., and Tawfik, D. S. (2005) Shared promiscuous activities and evolutionary features in various members of the amidohydrolase superfamily, *Biochemistry 44*, 12728−12736.
10. Seibert, C. M., and Raushel, F. M. (2005) Structural and catalytic diversity within the amidohydrolase superfamily, *Biochemistry 44*, 6383−6391.
11. Stover, C. K., Pham, X. Q., Erwin, A. L., Mizoguchi, S. D., Warrener, P., Hickey, M. J., Brinkman, F. S., Hufnagle, W. O., Kowalik, D. J., Lagrou, M., Garber, R. L., Goltry, L., Tolentino, E., Westbrock-Wadman, S., Yuan, Y., Brody, L. L., Coulter, S. N., Folger, K. R., Kas, A., Larbig, K., Lim, R., Smith, K., Spencer, D., Wong, G. K., Wu, Z., Paulsen, I. T., Reizer, J., Saier, M. H., Hancock, R. E., Lory, S., and Olson, M. V. (2000) Complete genome sequence of *Pseudomonas aeruginosa* PA01, an opportunistic pathogen, *Nature 406*, 959−964.
12. Borek, B. A., and Waelsch, H. (1953) The enzymatic degradation of histidine, *J. Biol. Chem. 205*, 459−474.
13. Magasanik, B., and Bowser, H. R. (1955) The degradation of histidine by *Aerobacter aerogenes*, *J. Biol. Chem. 213*, 571−80.
14. Tabor, H., and Rabinowitz, J. C. (1957) Formiminoglycine, formimino-L-aspartic acid, formimino-L-glutamic acid, *Biochem. Prep. 5*, 100−105.
15. Tabor, H., and Mehler, A. H. (1954) Isolation of N-formyl-L-glutamic acid as an intermediate in the enzymatic degradation of L-histidine, *J. Biol. Chem. 210*, 559−568.
16. Muszbek, L., Polgar, J., and Fesus, L. (1985) Kinetic determination of blood coagulation Factor XIII in plasma, *Clin. Chem. 31*, 35−40.
17. Nanba, H., Takaoka, Y., and Hasegawa, J. (2003) Purification and characterization of formate dehydrogenase from *Ancylobacter aquaticus* strain KNK607M, and cloning of the gene, *Biosci. Biotechnol. Biochem. 67*, 720−728.
18. Beutler, H.-O. (1990) L-Glutamate, colorimetric method with glutamate dehydrogenase and diaphorase, in *Methods of Enzymatic Analysis* (Bergmeyer, H. U., Ed.) 3rd ed., Vol. 8, pp 369−376, John Wiley & Sons, Inc.
19. Cleland, W. W. (1979) Statistical analysis of enzyme kinetic data, *Methods Enzymol. 63*, 103−138.
20. Hu, L., and Phillips, A. T. (1988) Organization and multiple regulation of histidine utilization genes in *Pseudomonas putida*, *J. Bacteriol. 170*, 4272−4279.
21. Ireton, G. C., McDermott, G., Black, M. E., and Stoddard, B. L. (2002). *J Mol. Biol. 315*, 687−697.
22. Wilson, D. K., and Quiocho, F. A. (1993) A pre-transition-state mimic of an enzyme: X-ray structure of adenosine deaminase with bound 1-deazaadenosine and zinc-activated water, *Biochemistry 32*, 1689−1694.
23. Wang, Z., and Quiocho, F. A. (1998) Complexes of adenosine deaminase with two potent inhibitors: X-ray structures in four independent molecules at pH of maximum activity, *Biochemistry 37*, 8314−8324.

BI0525425